Available online at www.sciencedirect.com
SCIENCE DIRECT®
Tectonophysics 373 (2003) 55–73
TECTONOPHYSICS
www.elsevier.com/locate/tecto

Salt redistribution during extension and inversion inferred from 3D backstripping

Magdalena Scheck*, Ulf Bayer, Björn Lewerenz

GeoForschungsZentrum Potsdam, Albert-Einstein-Strasse, Telegrafenberg Haus C, 14473 Potsdam, Germany

Received 25 October 2001; accepted 26 September 2002

Abstract

A 3D backstripping approach considering salt flow as a consequence of spatially changing overburden load distribution, isostatic rebound and sedimentary compaction for each backstripping step is used to reconstruct the subsidence history in the Northeast German Basin. The method allows to determine basin subsidence and the salt-related deformation during Late Cretaceous–Early Cenozoic inversion and during Late Triassic–Jurassic extension. In the Northeast German Basin, the deformation is thin-skinned in the basinal part, but thick-skinned at the basin margins. The salt cover is deformed due to Late Triassic–Jurassic extension and Late Cretaceous–Early Cenozoic inversion whereas the salt basement remained largely stable in the basin area. In contrast, the basin margins suffered strong deformation especially during Late Cretaceous–Early Cenozoic inversion. As a main question, we address the role of salt during the thin-skinned extension and inversion of the basin. In our modelling approach, we assume that the salt behaves like a viscous fluid on the geological time-scale, that salt and overburden are in hydrostatical near-equilibrium at all times, and that the volume of salt is constant. Because the basement of the salt is not deformed due to decoupling in the basin area, we consider the base of the salt as a reference surface, where the load pressure must be equilibrated. Our results indicate that major salt movements took place during Late Triassic to Jurassic E–W directed extension and during Late Cretaceous–Early Cenozoic NNE–SSW directed compression. Moreover, the study outcome suggests that horizontal strain propagation in the salt cover could have triggered passive salt movements which balanced the cover deformation by viscous flow. In the Late Triassic, strain transfer from the large graben systems in West Central Europe to the east could have caused the subsidence of the Rheinsberg Trough above the salt layer. In this context, the effective regional stress did not exceed the yield strength of the basement below the Rheinsberg Trough, but was high enough to provoke deformation of the viscous salt layer and its cover. During the Late Cretaceous–Early Cenozoic phase of inversion, horizontal strain propagation from the southern basin margin into the basin can explain the intensive thin-skinned compressive deformation of the salt cover in the basin. The thick-skinned compressive deformation along the southern basin margin may have propagated into the salt cover of the basin where the resulting folding again was balanced by viscous salt flow into the anticlines of folds. The huge vertical offset of the pre-Zechstein basement along the southern basin margin and the amount of shortening in the folded salt cover of the basin indicate that the tectonic forces responsible for this inversion event have been of a considerable magnitude.

Keywords: Basin inversion; Salt tectonics; Backstripping; Basin modelling; North German Basin; North Central Europe; Southern Permian Basin

* Corresponding author. Tel.: +49-331-288-13-45; fax: +49-331-288-13-49.
E-mail addresses: leni@gfz-potsdam.de (M. Scheck), bayer@gfz-potsdam.de (U. Bayer), lew@gfz-potsdam.de (B. Lewerenz).

0040-1951/$ - see front matter © 2003 Elsevier B.V. All rights reserved.
doi:10.1016/S0040-1951(03)00283-X

1. Introduction

Salt movement during the deformation of sedimentary basins under changing stress fields can have a strong impact on the localisation of subsidence centres, of faults and folds, on the distribution of facies and on the thermal field. However, the salt geometry at certain times in basin history is very difficult to quantify. Various techniques are applied to understand and quantify the influence of salt movements, and studies evaluating different restoration techniques have been validated on a wide range of structures (e.g. Rowan, 1993; Stewart et al., 1996; Zirngast, 1996; Schäfer et al., 1998). Commonly, subsidence history studies involve backstripping of the stratigraphic units deposited in a basin. Thereby, the influence of isostatic loading and of sediment compaction due to loading is removed for every stratigraphic unit to derive the amount of tectonic subsidence and finally paleotopographic information (Steckler and Watts, 1978; Sclater and Christie, 1980; Bond and Kominz, 1984). Backstripping in basins influenced by salt tectonics requires redistribution of the salt that migrated at different times to derive correct quantifications of subsidence history. This implies that it is necessary to know the shape of the salt layer at the respective stages of basin history to understand the factors controlling basin evolution.

Here, we present a 3D backstripping approach considering salt flow as a consequence of spatially changing overburden load distribution, isostatic rebound and sedimentary compaction for each backstripping step. The method has been developed in the course of subsidence analysis and basin modelling in the Northeast German Basin (NEGB) for which a 3D structural model has been used. The NEGB comprises the eastern part of the North Sea–North German Basin salt province (Fig. 1) which is structurally influenced by the mobilized Upper Permian Zechstein salt. It developed in an intracontinental setting as a subbasin of the Southern Permian Basin (Ziegler, 1990; Van Wees et al., 2000) and contains about 57,000 km^3 of Upper Permian Zechstein salt deposited in up to seven evaporite cycles, with anhydrite to halite precipitates and marginal carbonate platforms (Kiersnowski et al., 1995). The Mesozoic to Cenozoic cover of the salt is up to 5 km thick and the internal structure the NEGB is strongly determined by the distribution of salt diapirs and pillows. Like in many salt-containing basins, the salt layer acted as a decoupling horizon during post-depositional phases of deformation and thus played an important role in the subsidence history.

It is well known that viscous salt layers exert a strong influence on deformation geometry in the cover layers. Deformation geometry may vary in response of the direction and magnitude of regional stress as well as of the mechanical properties of the sedimentary layers or the thickness ratios between salt and cover (e. g. Vendeville and Jackson, 1992; Schultz-Ela et al., 1993; Vendeville et al., 1995; Stewart et al., 1996). When cover deformation and diapir location are directly linked to basement faults, commonly the term thick-skinned is used, while the term thin-skinned refers to structural settings where the salt detaches its cover from the basement and basement faults are absent or show no direct relation to cover deformation (e.g. Vendeville and Jackson, 1992; Demercian et al., 1993; Odonne and Costa, 1993; Stewart et al., 1996). Within this nomenclatoric frame, the deformation is thin-skinned in the basinal part of the NEGB but is thick-skinned at the basin margins. We aim to evaluate the relationship between the distribution pattern of salt structures and different tectonic processes that affected the NEGB since the Mesozoic.

2. Geological setting

The present distribution of salt structures in the Southern Permian Basin (Fig. 1) is characterised by the dominance of two trends (Jaritz, 1987; Nalpas and Brun, 1993; Kockel, 1996; Lokhorst, 1998; Scheck et al., 2002). North of the Elbe Fault System, salt structures strike predominantly N–S and thus parallel to Mesozoic graben structures as the Glückstadt Graben (Kockel, 1996), the Horn Graben (Clausen and Korstgård, 1996) and the Central Graben (Cartwright, 1989; Cartwright et al., 2001). Along the Elbe Fault System and south of it, salt structures strike predominantly WNW–ESE and thus parallel to Late Jurassic–Early Cretaceous basins as the Broad Fourteens, the Sole Pit (Ziegler, 1990; Nalpas and Brun, 1993) and the Lower Saxony Basins (Betz et al., 1987) which were inverted during Late Cretaceous–Early Tertiary (Ziegler, 1990). This spatial correspon-

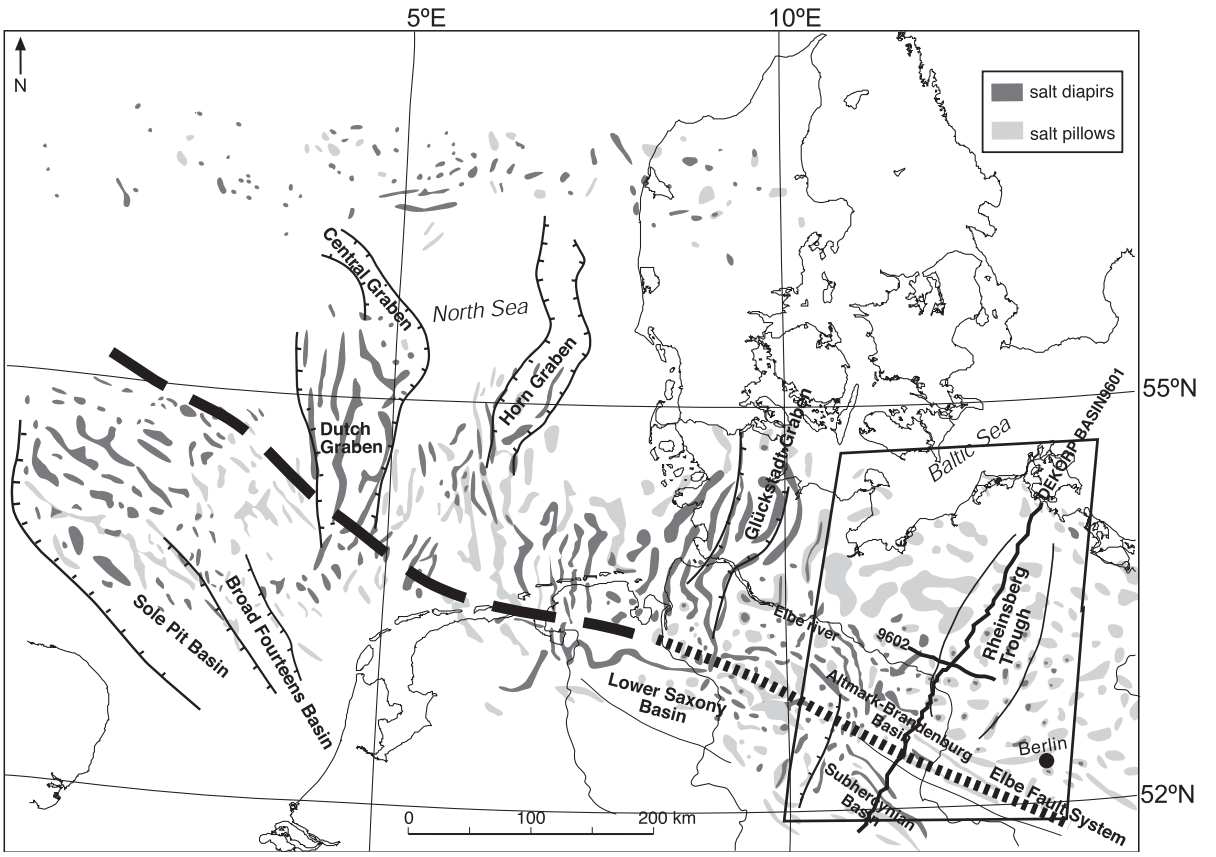

Fig. 1. Position of the study area in the salt province of North Central Europe (after Jaritz, 1987; Nalpas and Brun, 1993; Remmelts, 1995; Kockel, 1996; Lokhorst, 1998; Scheck et al., 2002). The model of the Northeast German Basin covers the area enclosed by the rectangle in the eastern part of the Southern Permian Basin. The Elbe Fault System (EFS, thick black dashed line) separates the salt structures of North Central Europe into a province of NNE- to N-trending salt structures in the north and a province of NW- to WNW-oriented salt structures in the south. Lambert Conformal Conic Projection.

dence between salt structures and tectonic elements points towards a causal link between them.

In the NEGB, the major tectonic phases were controlled by the regional stress field of North Central Europe. Basin initiation in Late Carboniferous–Early Permian was influenced by thermal destabilisation of the lithosphere and by post-Variscan wrenching (Benek et al., 1996). The initial rift-phase was followed by a phase of thermal subsidence in the Southern Permian Basin with a WNW–ESE directed basin axis extending form the Southern North Sea to Poland (Van Wees et al., 2000). In Middle–Late Triassic times, E–W directed extension led to differentiation of the Permian Basins with formation of northerly striking graben structures in North Central Europe. This is documented by accelerated subsidence and active normal faulting, e.g. in the Glückstadt Graben: (Kockel, 1996; Jaritz, 1987) and in the Central and Horn Grabens (Ziegler, 1990; Nalpas and Brun, 1993; Kockel, 1995; Stewart et al., 1996; Hooper and More, 1995; Remmelts, 1995; Buchanan et al., 1996; Clausen and Pedersen, 1999). In the NEGB, the NNE–SSW striking Rheinsberg Trough developed in Late Triassic perpendicular to regional extension (Scheck and Bayer, 1999).

During Jurassic times, a rotation of depocentral axes from ±N–S (Triassic) to NW–SE occurred along the southern margin of the former Southern Permian Basin, possibly due to a transtensional tectonic regime (Ziegler, 1990). This is documented by

increased subsidence in the Broad Fourteens Basin, in the Sole Pit Basin (Nalpas and Brun, 1993) and in the Lower Saxony Basin (Betz et al., 1987). In the NEGB, accelerated Late Jurassic–Early Cretaceous subsidence is documented in the WNW–ESE striking Subhercynian and Altmark–Brandenburg Basins (Schwab, 1985; Scheck and Bayer, 1999). In Late Cretaceous–Early Tertiary, North Central Europe was affected by compression induced by the Alpine convergence which led to inversion in the Central European Basin System (Badley et al., 1989; Coward and Stewart, 1995; Hooper and More, 1995; Remmelts, 1995; Buchanan et al., 1996; Stewart et al., 1996). Accordingly, Late Cretaceous–Early Cenozoic compression led to uplift and erosion in the NEGB with differential inversion along WNW–ESE striking structures in the southern part of the basin and along its margins. Finally, subsidence again affected large parts of the Central European Basin System during the Cenozoic and this is also documented by the sedimentary record of the NEGB.

3. Salt movements in the NEGB

Detailed studies of the NEGB showed that in this part of the Zechstein salt province, deformation of the salt cover is mechanically decoupled from deformation of the salt basement (Meinhold and Reinhardt, 1967; Schwab, 1985; Scheck and Bayer, 1999; Kossow et al., 2000; Scheck et al., 2002). Furthermore, basin-wide tectonic phases and pulses of salt mobilisation do correlate temporally. A change in orientation of salt structures is observed to correlate with changes of the regional stress field throughout the Mesozoic–Cenozoic and the axes of salt rim synclines rotate with time (Brink et al., 1992; Scheck et al., 2002).

The degree of tectonic decoupling in the basinal part of the NEGB is imaged by comparison of the modelled top and base salt surfaces (Fig. 2). The top salt surface (Fig. 2a) shows that the structure of the cover layers is controlled by narrow, tall diapirs with a structural amplitude of up to 4000 m surrounded by welds in the eastern and southern marginal part of the basin. Diapirs are aligned along axes parallel to the Elbe Fault System and to the Rheinsberg Trough. In contrast, the salt layer is almost undeformed over long distances in the northwestern part of the basin where only smooth, long-wavelength salt pillows are present. The base Zechstein surface (Fig. 2b) shows no major faults cutting the base Zechstein below the basinal area where this surface is smooth and lies about 5 km deep. The isolines trace a wide depression with a NW–SE directed axis. Only below the Rheinsberg Trough the 5000-m isoline shows a deviation into the trough direction. On the contrary, the vertical displacement of the pre-Zechstein basement amounts more than 5 km along the WNW–ESE striking Elbe Fault System at the southern basin margin. Some smaller faults are present at the northern basin margin.

The reflection seismic expression of this tectonic decoupling is imaged along the onshore profiles of the DEKORP BASIN'96 experiment (DEKORP-BASIN Research Group, 1999). Line BASIN9601 (Fig. 3a–d) is crossing the basin in a NNE–SSW direction, perpendicular to the strike of the Permo-Triassic basin axis and to the WNW–ESE striking inversion structures. While the salt cover is affected by folding and faulting across large parts of the basin, the salt basement shows almost no faulting in the area of the basin but is severely faulted along the basin margins. Basement deformation is most intense at the Elbe Fault System, where the base Zechstein is displaced by 2 Seconds Two Way Traveltime (s TWT) along the Gardelegen Fault (Fig. 3b). Some smaller basement faults are visible to about 50 km north of the Gardelegen Fault and at the northern margin. This observation of thin-skinned deformation is supported by a huge amount of seismic data of which only a small fraction has been published so far (e.g. Meinhold and Reinhardt, 1967; Hoffman and Stiewe, 1994; Kossow et al., 2000; Kossow, 2002; Scheck et al., 2002; Otto and Bayer, 2001). It might be a point of discussion if the absence of faults is due to the significant attenuation of seismic energy caused by the Zechstein evaporites. If this would be the case, the seismic image should be considerably better in areas where all the salt has been removed. This is not the case and the base Zechstein appears as a strong, continuous signal below salt-depleted areas as well as below salt pillows and diapirs (Fig. 3c,d; Kossow, 2002; Scheck et al., 2002). However, there could be small faults present the size of which is below seismic resolution, but even then the amount of deformation

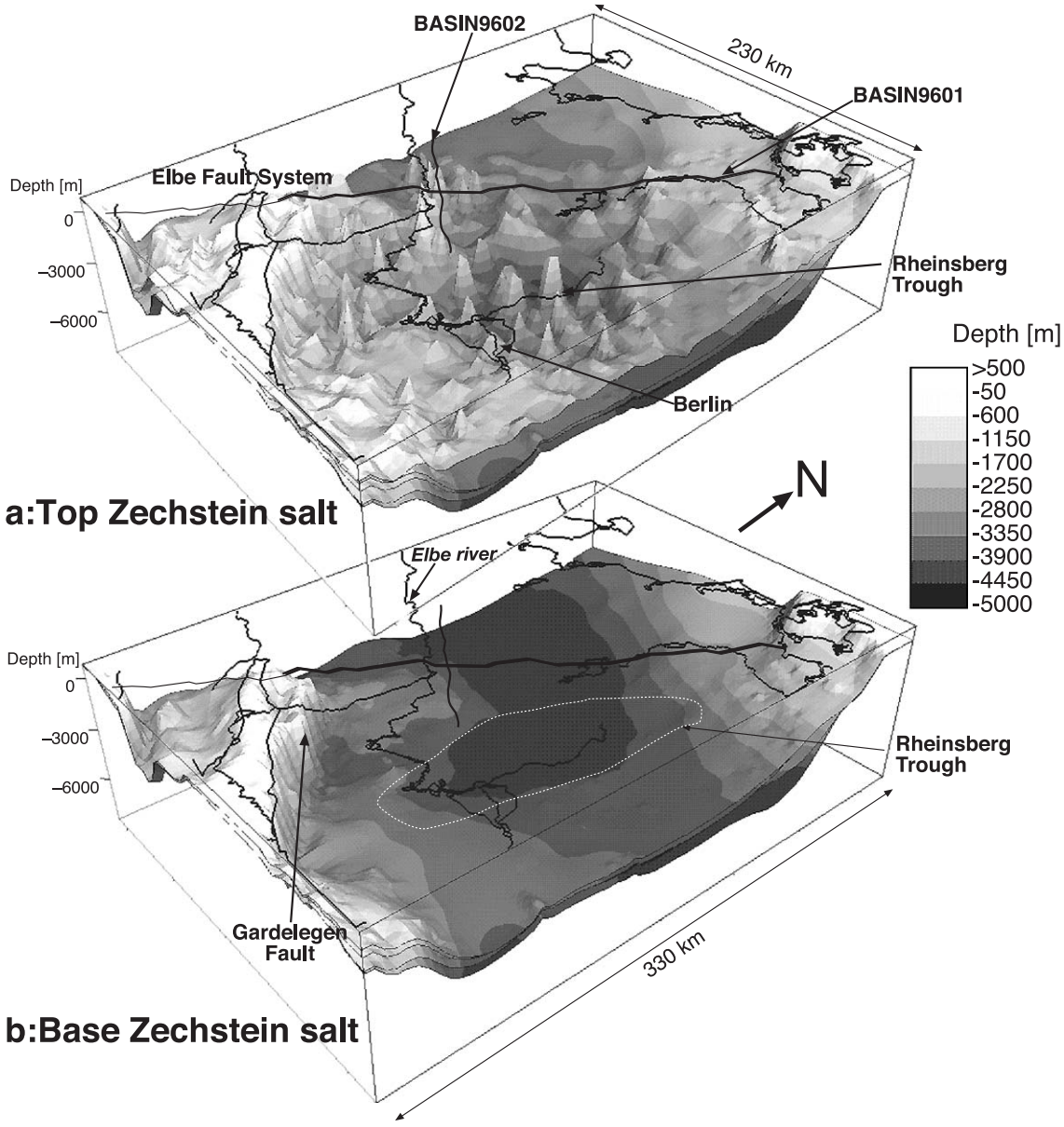

Fig. 2. View on the modelled top (a) and base (b) of the Upper Permian Zechstein salt layer in the Northeast German Basin illustrating a strong decoupling of deformation by the viscous salt. Salt diapirs are most mature along WNW–ESE oriented chains north of the Elbe Fault System and along NNE–SSW oriented axes in the area of the Rheinsberg Trough.

present in the salt basement is negligible small compared to the amount of deformation present in the salt cover or at the basin margins.

Above the salt layer the entire Mesozoic interval is folded with salt cored anticlines and salt-depleted synclines. The onset of salt mobilisation is observed

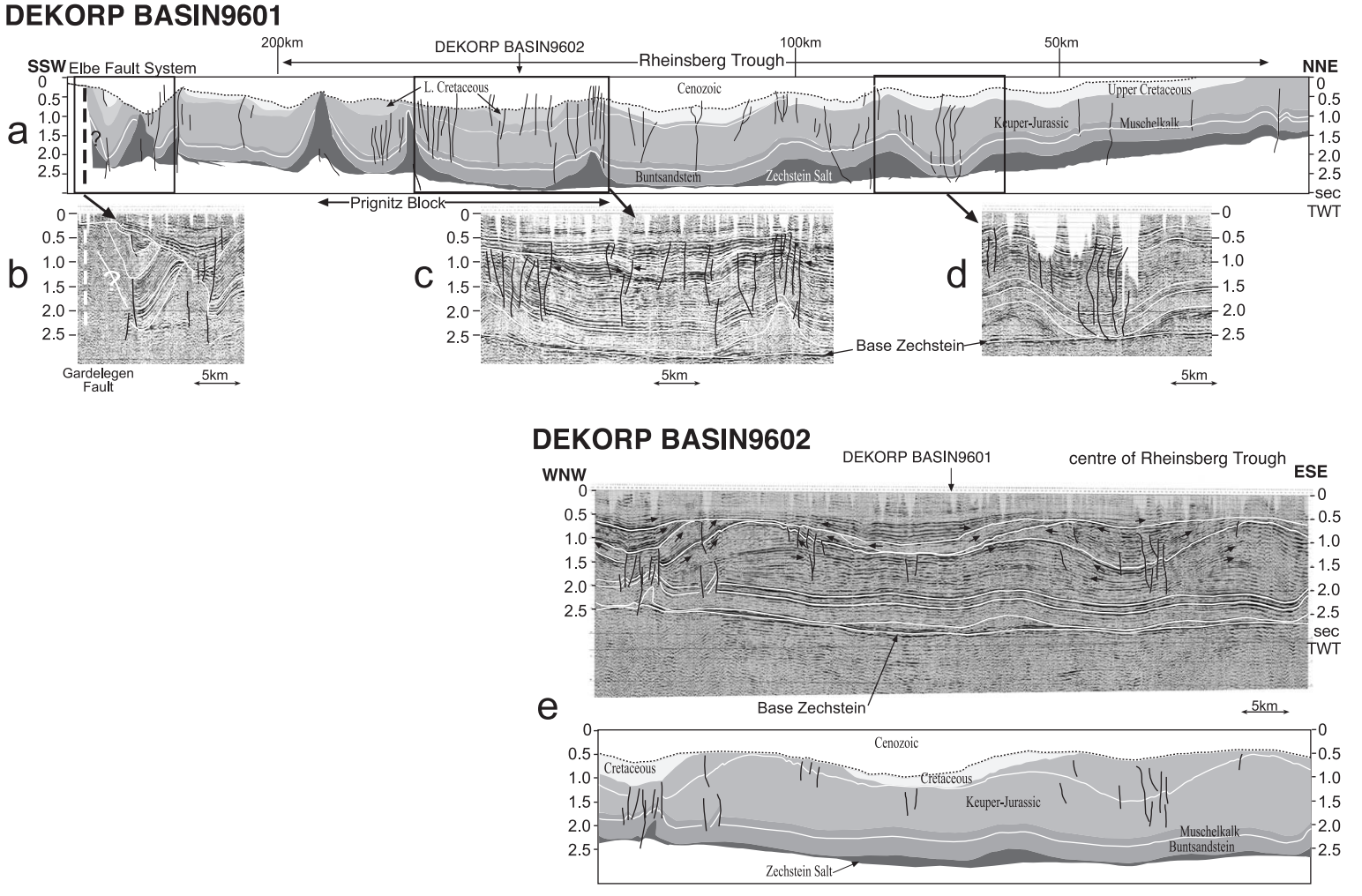

Fig. 3. (a) Interpretation of the BASIN9601 profile showing that the salt layer decouples a folded and faulted cover succession from an almost continuous, not faulted basement in the basinal areas. Basement deformation is localised at the southern basin margin, where the base Zechstein is displaced along the Elbe Fault System. A tighter folded Mesozoic interval is separated from a wider folded Cenozoic level by the erosive base Cenozoic unconformity. On the Prignitz Block pre-Cenozoic erosion affected deeper levels than north and south of it—an indication for differential uplift of this block during inversion. (b) Seismic detail from the Elbe Fault System showing syn-tectonic and/or syn-diapirism sequences in the Mesozoic and a change in subsidence regime in the Cenozoic. (c, d) Seismic details imaging stratigraphic thickening associated with normal faulting in the Mesozoic between salt structures. (e) Profile BASIN9602 perpendicular to the Rheinsberg Trough axis showing sequences in the Keuper–Jurassic interval between salt pillows that are syn-kinematic to salt withdrawal and are affected by normal faulting. Note the clear and continuous signal of the base Zechstein reflection below both: salt and areas depleted of salt. Arrows indicate terminating reflections.

synchronous with the development of the NNE–SSW striking Rheinsberg Trough in the Late Triassic Keuper. This is inferred from stratigraphic thickening near salt structures in the Keuper–Jurassic interval and associated synsedimentary normal faults (Fig. 3b–d). Both observations indicate rim syncline subsidence and extension during Keuper–Jurassic times. Line BASIN9602 (Fig. 3e) runs perpendicular to the axis of the Late Triassic Rheinsberg Trough. This line crosses the western shoulder of the trough in its southern part and ends to the east in the trough centre. It also demonstrates that the bundle of reflections interpreted as Late Triassic (Keuper)–Jurassic is thickening toward the trough centre and shows indications for syn-sedimentary salt movements in the reflective pattern. The salt is almost completely removed below the trough. While normal faults are present in the Mesozoic cover, the base Zechstein again appears as a strong, continuous signal below the trough. Only at the western end of the line, the salt basement is offset with about 0.15 s TWT along a Mesozoic normal fault. This scarcity of basement deformation below the Rheinsberg Trough is evident in many seismic sections crossing the Rheinsberg Trough (Meinhold and Reinhardt, 1967; Hoffman and Stiewe, 1994; Kossow et al., 2000; Scheck et al., 2002). Thus, the Rheinsberg Trough is not a true 'graben' but could represent a large salt rim syncline (about 200 km long in NNE–SSW direction and 70 km wide) below which the salt has been largely withdrawn and migrated into marginal diapirs.

The Late Jurassic–Early Cretaceous subsidence in the NW–SE striking Altmark–Brandenburg Basin also was accompanied by a phase of salt mobilisation and the former N–S striking salt rim synclines rotated into a NW–SE direction (Scheck et al., 2002). Salt movement continued during Cretaceous and Cenozoic times as indicated by rim syncline formation between salt diapirs and pillows (Fig. 3). Late Cretaceous–Early Cenozoic compression of the NEGB led to the development of folds with WNW–ESE striking axes in the southern part of the basin and to the differential uplift of blocks (e.g. Prignitz Block) bordered by salt diapirs and deep narrow salt rim synclines (Fig. 3a,b). This uplift of inverted blocks was again not accommodated by brittle failure of the salt basement in the basinal area (Kossow et al., 2000; Kossow, 2002; Scheck et al., 2002). A regional unconformity is truncating the Mesozoic interval, indicating erosion after the folding but prior to Cenozoic sedimentation. The youngest rocks affected by the folding event are Maastricht in age as well data indicate and the oldest rocks above the unconformity are dated as Mid–Early Paleocene (Hoth et al., 1993). Cenozoic salt rim synclines are present along both

Table 1

Time interval	Tectonic regime	Deformation pattern	Salt movements
Permian–Triassic	thermal subsidence	• WNW–ESE striking sag basin, • minor faulting	• stable salt
Late Triassic–Jurassic	Regional E–W Extension	• Subsidence of the NNE–SSW trending • Rheinsberg Trough • no basement faulting	• Syn-sedimentary uprise of Zechstein salt • Axes of salt structures strike ± N–S
Late Jurassic–Early Cretaceous	Trans-tension	• Uplift in the N, • WNW–ESE oriented • depocentres in the S • (Altmark–Brandenburg Basin)	• Syn-sedimentary uprise of Zechstein salt • Rotation of salt rim syncline axes to NW–SE
Late Cretaceous–Early Tertiary	NNE–SSW compression	• Folding of salt cover • uplift of WNW–ESE oriented blocks, • WNW–ESE striking basement faults only at the S′ margin	• Syn-sedimentary uprise of Zechstein salt • salt structures strike WNW–ESE
Late Cretaceous–Early Tertiary	Regional uplift	• erosional unconformity	
Cenozoic	Compression?	• Final Subsidence of the entire basin with the basin axis oriented WNW–ESE	• Continued salt uprise • Wavelength of structures larger than in Late Cretaceous times

BASIN'96 lines but their wavelength is considerably larger than that of the Mesozoic synclines.

In summary, the evaluation of the tectonic phases of the NEGB and the phases of salt movements (Table 1) revealed that both correlate temporally and that neither Late Triassic extension nor Late Cretaceous–Early Cenozoic compression resulted in considerable brittle failure of the basement in the basin area. The question rising from these observations is: Did the salt motion passively balance the major part of extension and compression in the basin area by viscous flow? If this was the case, then backstripping and the reconstruction of salt movements should lead to a reconstruction of deformation in the basin area and it should be possible to model the salt movements related to the different deformation stages. We address this question by using 3D backstripping considering salt redistribution.

4. Backstripping method

Although much is known about salt tectonic deformation principles, it is still a major problem to apply this knowledge in backstripping procedures concerning the subsidence history. Backstripping techniques applied to salt-containing basins commonly are performed as 2D restorations of depth converted seismic sections (e.g. Rowan, 1993; Stewart et al., 1996; Zirngast, 1996; Schäfer et al., 1998). Modern examples consider physical processes associated with backstripping as decompaction of unloaded sediments, restoration of fault displacements and isostatic rebound (e.g. Schäfer et al., 1998; Buchanan et al., 1996). A new 2D approach presented by Ismail-Zadeh et al. (2001) combines backstripping with salt restoration assuming different rheologies for the salt and its overburden layers. A major shortcoming of 2D restorations is that salt movements perpendicular to the plane of cross section cannot be quantified and constrained. Only a few examples exist where 3D restoration has been applied to salt containing basins. As a common feature these studies assume a balance between downbuilding and salt withdrawal. They relate the thickness of the diapirs' peripheral sinks to the amount of salt withdrawn from the corresponding area (Zirngast, 1996) or assume a balance between the amount of salt migration and the amount of sediments deposited when the effects of isostatic loading, sedimentary compaction and erosion are removed (Schäfer et al., 1998; Yin and Groshong, 1999; Whitefield et al., 1999). Generally, 3D restorations are applied to areas of relatively limited extent including a small number of diapirs and not balancing the total salt volume in the basin as the restoration procedures involve long calculation times.

We are aware that the present distribution of salt is the result of a complex interaction between the viscous behavior of salt and an elasto-plastic behaviour of surrounding layers. For this reason, backstripping of salt layers is not trivial in a mathematical sense as there is no definite path to reconstruct the entire history of a deformed viscous layer. Nevertheless, as backstripping is an inverse method, salt motion can also be considered invertable by introducing certain simplifications. We propose a simple approach considering the motion of salt as invertable for each backstripping step. The method allows to redistribute the salt in 3D in response to the actual overburden, while conserving the volume. We apply the method on the 3D structural model of the Northeast German Basin, with two major goals: (1) to quantify the role of salt during the deformation history of the basin, and (2) to model the salt movements related to the different deformation stages.

4.1. Observations to be considered and basic assumptions

In our modelling approach, we make some basic assumptions. First, we assume that the salt behaves like a viscous fluid on geological time-scales. This is consistent with the outcome of many studies related to the complexity of salt tectonic deformation (e.g. Vendeville and Jackson, 1992; Schultz-Ela et al., 1993; Davison et al., 1995), with analogue modeling studies (e.g. Koyi et al., 1993; Nalpas and Brun, 1993; Vendeville et al., 1995) and with results from numerical models (van Keken et al., 1993; Poliakov et al., 1993; Podlachikov et al., 1993), which all indicate that salt reacts as a viscous fluid over geological time spans.

The second assumption is that salt and overburden are in hydrostatical near-equilibrium at all times, which means that the shape of the salt upper surface

is dependent of the load acting on it. This is consistent with the observation of a balance between the thickness of the diapirs' peripheral sinks and the amount of salt withdrawn from the corresponding area (e.g. Zirngast, 1996).

As a third assumption, we consider the volume of salt to be constant because we treat the salt as an incompressible fluid and seismic data indicate that almost no salt is lost due to solution in the NEGB.

Fourth, we use the observation that the deformation is tectonically decoupled by salt in the basin area of the NEGB as an additional constraint. Knowing that the basement of the salt is almost not deformed due to decoupling enables us to consider the base of the salt as a reference surface, where the load pressure must be equilibrated.

4.2. Modelling concept

Prior to backstripping, we define a starting model with assigned physical properties for the different sedimentary layers including load-porosity-dependent densities and associated compaction. This 3D structural model corresponds to the model described by Scheck et al. (1999) and is based on thickness and depth maps (ZGI, 1968–1990) in addition to the data of 63 deep wells (5–8 km) published by Hoth et al. (1993) and some wells provided by Erdöl Ergas Gommern. It has been constructed using the Geological Modelling System (GMS, developed at the GeoForschungsZentrum Potsdam). Vertical resolution of the model corresponds to the number of stratigraphic units here: 12 layers representing Uppermost Carboniferous to Cenozoic-aged deposits. Horizontal resolution is approximately 4 km. Besides geometric information, every layer has assigned physical properties that are considered constant within the layer. Consequently, every layer is characterised by an average dominant lithology with lithology-dependent physical properties.

For this starting model we determine the sedimentary load using a 3D finite element method (Scheck and Bayer, 1999). For the resulting model of load distribution, we calculate a crustal density variation that is in isostatic equilibrium with the sediment load and the position of the Moho known from other sources (Rabbel et al., 1995; Giese, 1995; DEKORP-BASIN Research Group, 1999), assuming Pratt-Isostacy; this means we calculate which average density distribution

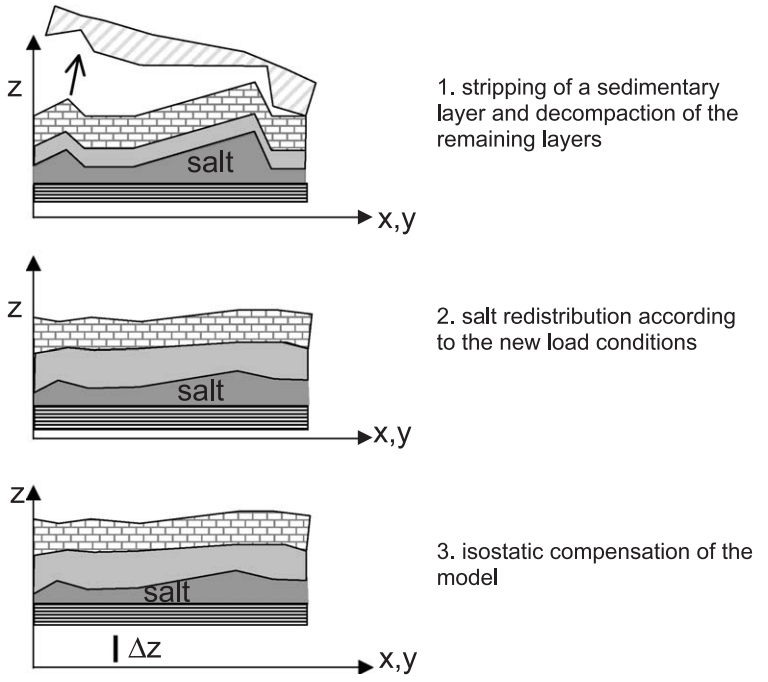

Fig. 4. Simplified scheme of the modelling concept to perform backstripping with salt redistribution.

in the crystalline crust would be in isostatic equilibrium with a given Moho position and a given sediment load (Scheck and Bayer, 1997, 1999). Subsequently, we stepwise remove the different stratigraphic layers and recalculate the salt distribution and the isostatic equilibrium according to an Iceberg Model for each step. After stripping of each layer, load-porosity-dependent densities and associated decompaction are recalculated (Scheck and Bayer, 1999).

Calculations are performed with software developed at the GeoForschungsZentrum Potsdam running on UNIX workstations or on LINUX-PCs. In order to handle the backstripping problem in a reasonable calculation time or even interactively, certain constraints have to be met during backstripping, and the complexity of 3D calculations has to be reduced. The 3D problem therefore is split into a stepwise solution of three separate processes (Fig. 4). The first step consists of stripping of a sedimentary layer and the decompaction of the remaining layers. Secondly, the salt is redistributed according to the new load conditions and the compaction distribution is adjusted again. Finally, the whole model is isostatically compensated.

The equilibrium distribution of salt is found for each backstripping step in an iterative process by alternating between salt redistribution and compaction adjustment followed by local isostatic compensation (backstripping).

Using the basic assumptions, the system is statically defined. Then, the load pressure at the base of the salt must be equilibrated. Pressure balancing affects only the upper surface of the salt and the overburden layers (Fig. 5). The pressure at the base of the salt $P(t)$ is the sum of the pressure acting on the salt upper surface $P_{\mathrm{top}}(t)$ (load of overburden sediments), and the load of the salt column $g\rho_s h_s(t)$ (Fig. 5a).

$$P(t) = P_{\mathrm{top}}(t) + g\rho_s h_s(t) \tag{1}$$

where g is gravity acceleration, ρ_s is the salt density and h_s is the height of the salt column (salt thickness) at a certain time t.

Under hydrostatic conditions (Fig. 5b), the pressure difference ΔP is zero within the salt between two points 1 and 2, at the same depth z_n:

$$\Delta P_{[1,2]}(t) = 0 = P_1(t) - P_2(t) + g\rho_s(h_1 - h_2) \tag{2}$$

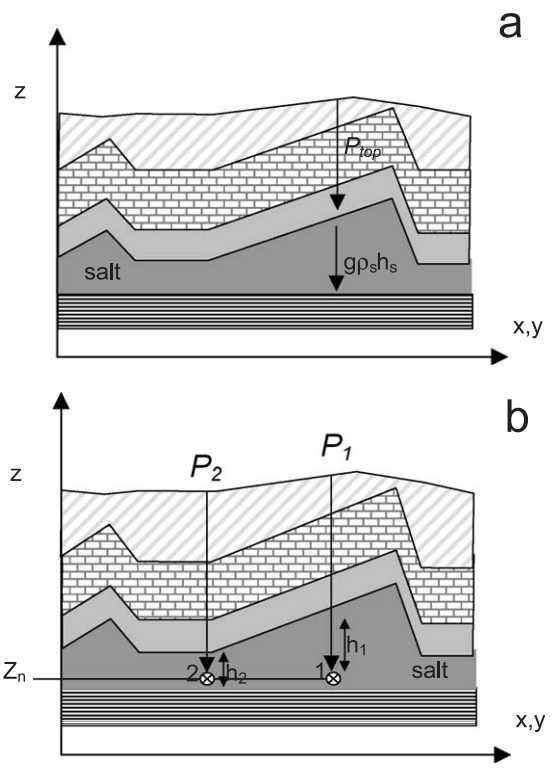

Fig. 5. Concept of load pressure distribution in the viscous salt layer in isostatic equilibrium. (a) The pressure at the salt base is the sum of the load acting on the salt surface and the load of the salt column. (b) The pressure difference between two points in the viscous medium or at the base of salt equals zero if they are at the same depth z_n.

Considering a relief of the base salt surface (Fig. 6a), Eq. (2) becomes:

$$\Delta P_{[1,2]}(t) = 0 = P_1(t) - P_2(t) + g\rho_s(h_1 - h_2) - (z_1 - z_2)g\rho_s \tag{3}$$

with the additional term '$-(z_1 - z_2)g\rho_s$' representing the reference depth of the base salt between the two points due to their absolute difference in depth, which is needed for isostatic balancing.

After removal of each layer, this condition ($\Delta P = 0$) is not accomplished as the load changes. Then, the salt has to be redistributed untill the above condition is true again. Therefore, we introduce a formal flux of salt j (Fig. 6b) that takes place to equilibrate the system with:

$$j = \Delta(P_{\mathrm{top}}(t) + g\rho h(t) + g\rho Z_{\mathrm{base}}) \tag{4}$$

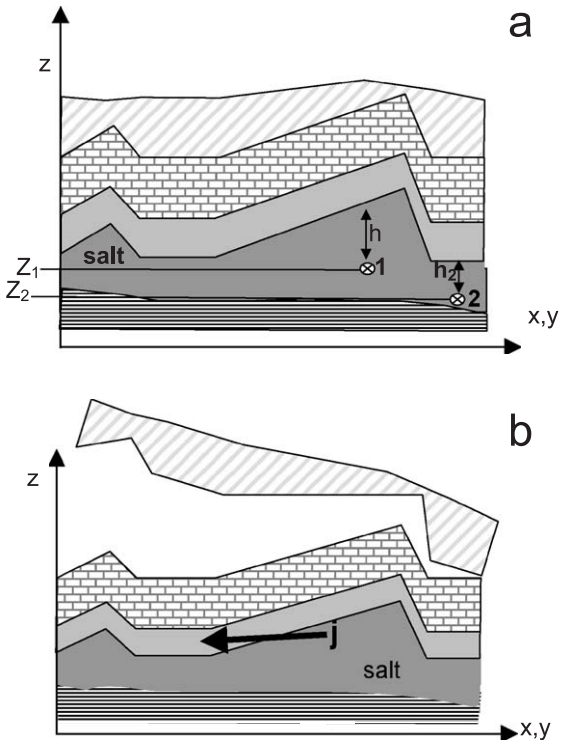

Fig. 6. (a) Concept for pressure balancing if the base salt is characterised by a topography. Points at the base salt at different depths are related to a reference depth for calculation. (b) Concept of salt redistribution. After stripping of a cover layer, a formal flux j is introduced to allow flow of salt towards areas of load deficit.

with

$$g\rho Z_{\text{base}} = -(z_i - z_{i+1})g\rho_s.$$

The objective is to find the salt thickness $h(x,y)$ corresponding to a flux $j(x,y)=0$.

New values of h are calculated iteratively in an explicit procedure by considering the fluxes over element boundaries with the surface area approximated by $h_{\Delta x \Delta y}$.

$$h_{i+1} = h_{i-1} + c\sum h_{iji},$$

where i indicates the fluxes over the different boundaries of an element, with c an arbitrary constant. Volume is preserved by observing that $j_{\text{out}}=j_{\text{in}}$ for two adjacent elements (divergence theorem). The boundaries of the area under consideration are kept closed (no flux condition).

In case the salt does not fill the entire basin, we allow moving boundaries, which are automatically introduced by considering a minimum salt thickness h_i close to zero. Once this value is achieved, the point is excluded from subsequent calculations and no salt can flow back to this point again. Thus, the salt that migrated from the basin centre to the basin margins during basin history can flow back into the deeper parts of the basin during reconstruction. Additionally, this value prevents the system to produce negative thicknesses as a consequence of the explicite method.

$h_i = 0$ for $h_i > h_{\min}$ which yields $h_{iji} = 0$.

A second value defines the minimum salt thickness where no salt can move away from but a further flow in is allowed. This value $h_{\text{minflow}} > h_{\min}$ allows refilling of areas from where the salt has been withdrawn during basin history.

Starting with the present-day model, we stepwise strip back all layers down to the top of the salt. After several iterations of smoothing the salt and final isostatic compensation of the model, we get the salt distribution for each step that is in hydrostatic equilibrium with the load of the overburden. Continued backstripping, followed by salt redistribution down to the top of Zechstein results in an equilibrated salt layer.

One major problem during the first tests of the method is imaged in Fig. 7a. It concerns the post-depositional piercing of more than one sedimentary layer by diapirs. When the last layer above the diapir is removed, the load above the diapir becomes zero. A viscous medium in hydrostatic equilibrium will not change its position anymore if no load is acting above. Therefore piercing cannot be reversed until the last layer is removed and the 'no load' condition applies for the whole salt surface. Correct solutions therefore are obtained by the described method only for the initial salt thickness and for salt pillows.

We tested different strategies to find an approximate solution for diapirs. One possible way is to integrate a primary thickness of the cover layers for each backstripping step and to load the system with this initial thickness to redistribute the salt. The concept is illustrated schematically in Fig. 7b. This means a set of initial thickness maps is needed for each backstripping step and thus the time of piercing

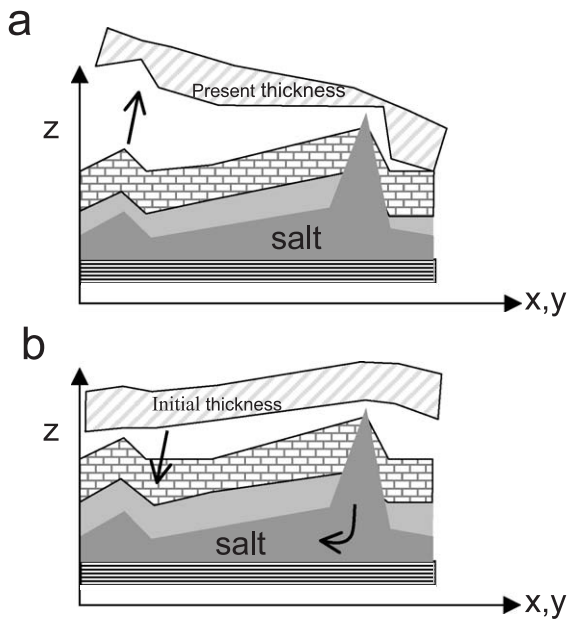

Fig. 7. (a) Problem of salt diapirs piercing several cover layers: removal of cover layers will not change the load above the diapir until the last layer is removed. For the time steps between, the salt movement can not be reversed with a unique solution. (b) Strategy to overcome the problem illustrated in (a). The integration of appropriate primary cover thickness during the backstripping procedure yields new load conditions corresponding to the respective time step and thus leads to salt redistribution.

enters the calculations as an additional model input. The respective thicknesses of the cover layers have to be derived by complementary geological methods, especially from seismic interpretation. In the case of the NEGB, we know that although salt uprise started in Late Triassic, the major phase of diapirism was in Late Cretaceous and Cenozoic times (Meinhold and Reinhardt, 1967; Schwab, 1985; Scheck et al., 2002). In addition, we used a published set of initial thickness maps (ZGI, 1968–1990) to reconstruct initial thicknesses. The latter were used to load the system during backstripping.

In Fig. 8, the modeled present-day thickness of the Mesozoic layers are illustrated in comparison with the reconstructed thickness maps. Facies distribution (Musstow, 1976) indicates that the Upper Cretaceous chalks were deposited over the entire basin area prior to the phase of strongest salt diapirism and were eroded after inversion. This is partly constrained by seismic data (Scheck et al., 2002). As we had no further information, we assumed a minimum of 250 m of eroded Upper Cretaceous on the crest of inverted blocks (Fig. 8a compared to Fig. 8b), which corresponds approximately to the smallest drilled thickness of Upper Cretaceous in the NEGB. The reconstruction of the other Mesozoic layers is based on published maps (ZGI, 1968–1990), on well data and on seismic interpretation (Scheck et al., 2002). The main difference between initial and present-day thickness (Fig. 8c–l) is that post-Early Cretaceous diapiric piercing caused holes in the pre-Cretaceous Mesozoic layers. Therefore, the present-day thickness of the Triassic and Jurassic layers is characterised by holes due to post-deposional piercing by salt diapirs. In the reconstructed thickness maps, these holes are closed and only the large-scale thickness distribution is matched. The basin-wide subsidence trend changes from a NW–SE oriented sag basin in Early Triassic Buntsandstein (Fig. 8l) and Muschelkalk (Fig. 8j) to a NNE–SSW oriented linear trough (Rheinsberg Trough) in Late Triassic (Fig. 8h) and Jurassic (Fig. 8f) and to WNW–ESE striking depocentres in Early Cretaceous (Fig. 8d).

5. Results

Fig. 9 shows the modelled thickness of Zechstein salt for the present-day state and for different stages of backstripping. In the model of present-day structure (Fig. 9a), the salt is distributed asymmetrically with tall diapirs in the southern and eastern half of the basin and smooth, long-wavelength salt pillows in the northwestern basin centre. Salt structures are aligned parallel to the Elbe Fault System in the south and along NNE–SSW striking axes in the area of the Rheinsberg Trough. Backstripping of the Cenozoic layer results in a change in salt distribution geometry. Once the load of the Cenozoic salt rim synclines is removed, the salt is flowing back to these areas. This results in a reduced number of diapiric structures especially in the northwestern part of the basin as imaged in Fig. 9b. Reloading the system with the reconstructed Mesozoic thickness distribution interpreted for the time prior to erosion and prior to diapiric piercing results in the salt distribution imaged in Fig. 9c. The major part of the diapirs is reduced to salt walls and pillows concentrated in the southern and eastern part of the basin. The

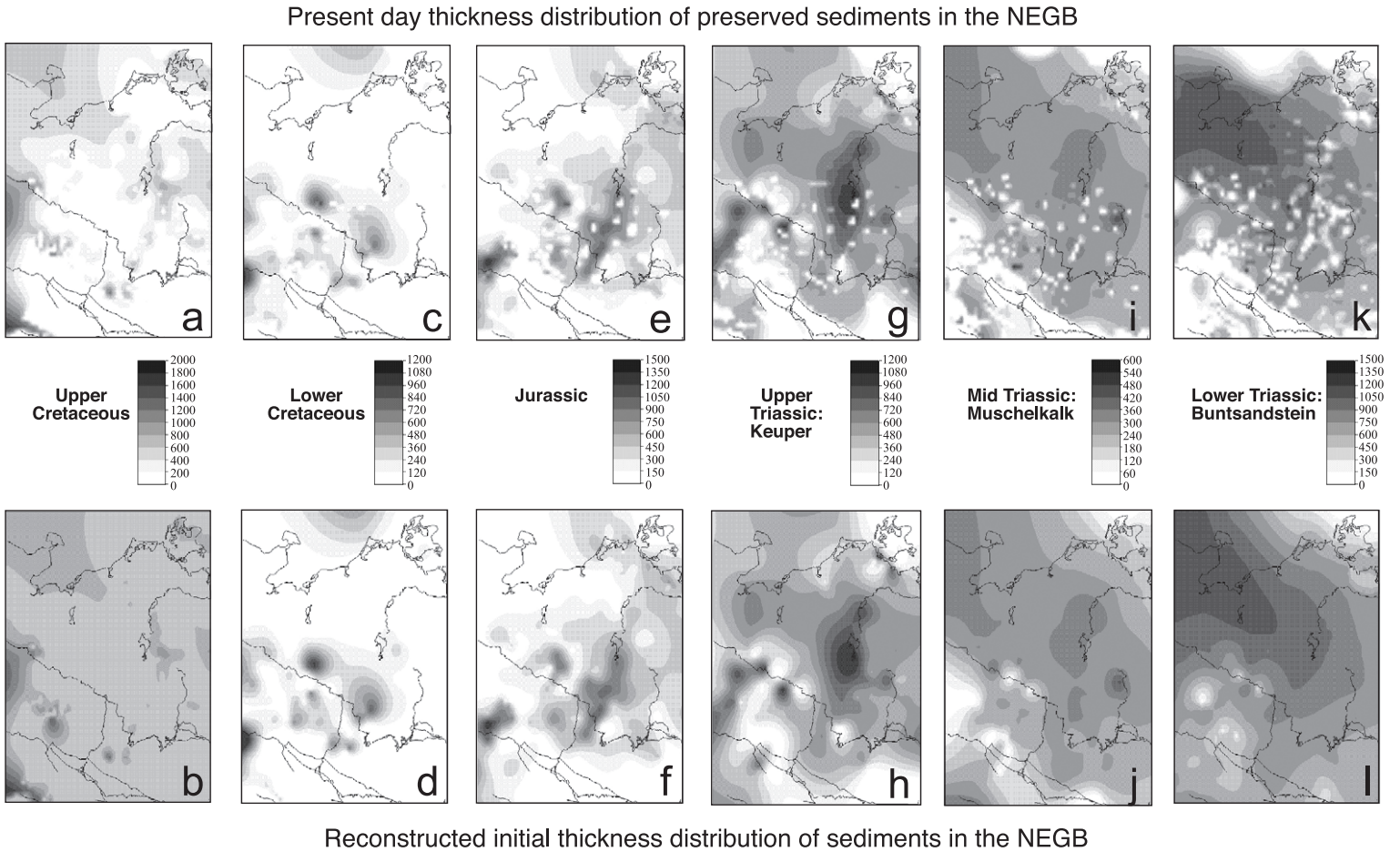

Fig. 8. Present-day isopach maps [in m] of the geologic units integrated in the 3D structural model of the NEGB (a, c, e, g, i and k). Small circular minima in the maps (white spots) are due to post-depositional salt piercing. In the reconstructed isopach maps (b, d, f, h ,j and l), the holes due to salt piercing are closed according to additional data and were used to reload the system after backstripping to the time prior to inversion.

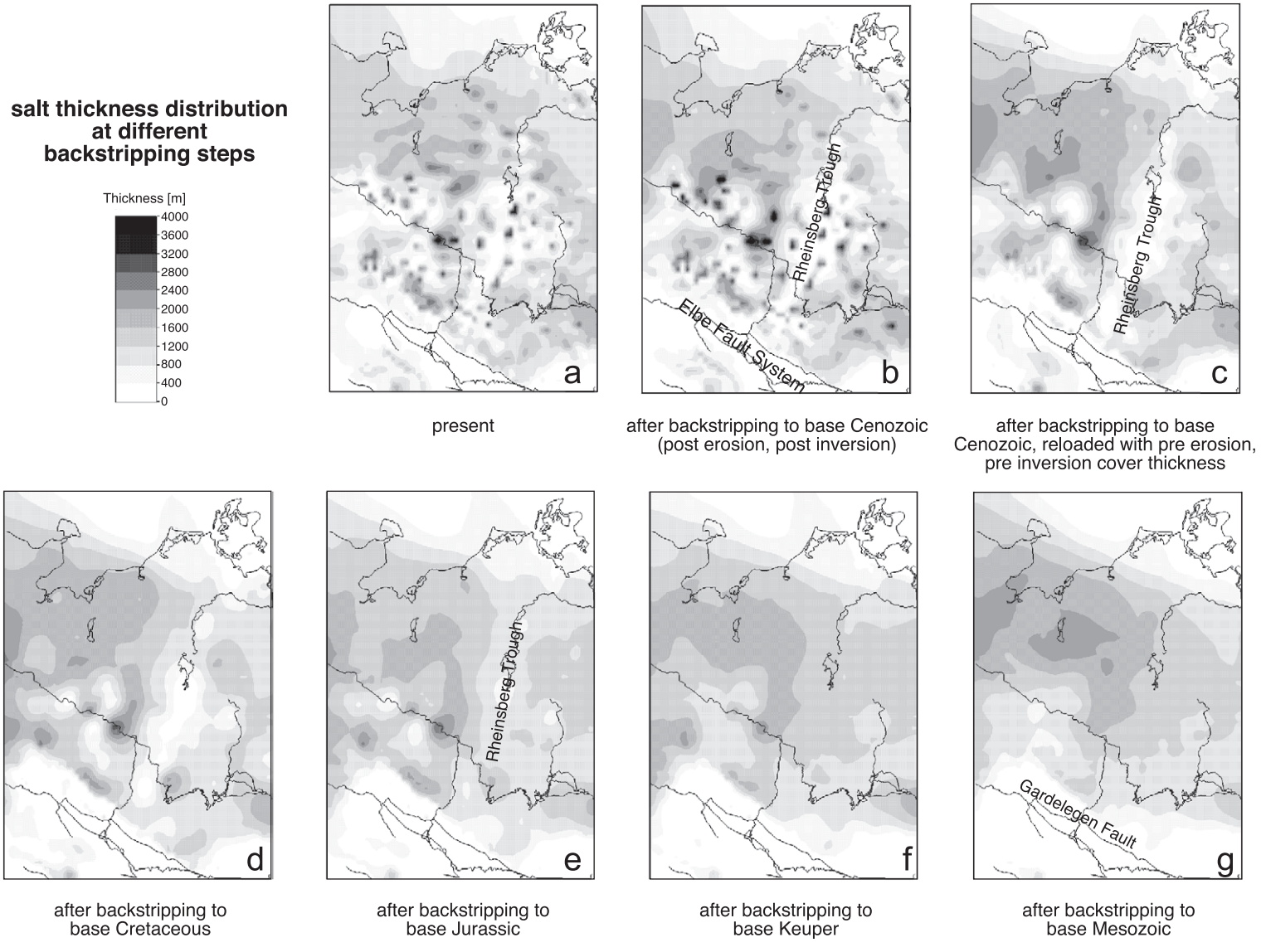

present

after backstripping to base Cenozoic (post erosion, post inversion)

after backstripping to base Cenozoic, reloaded with pre erosion, pre inversion cover thickness

after backstripping to base Cretaceous

after backstripping to base Jurassic

after backstripping to base Keuper

after backstripping to base Mesozoic

NNE–SSW striking Rheinsberg Trough is imaged as a linear hole in the salt layer, from where the salt has been withdrawn. This hole is flanked to the east by several salt structures aligned parallel to the eastern trough shoulder and to the west by a large NNE–SSW striking salt wall along the western trough shoulder. In the southern part of the basin, several openings in the salt layer are visible corresponding to the Cretaceous rim synclines.

The latter partly disappear after backstripping to the base Lower Cretaceous as imaged in Fig. 9d. The removal of the load corresponding to the Cretaceous rim synclines results in a redistribution of the salt to these areas. Additionally, the individual salt structures flanking the Rheinsberg Trough to the east in the previous backstripping step merge into a NNE–SSW striking, elongated salt wall. Backstripping to the base Jurassic (Fig. 9e) leads to further salt redistribution resulting in salt structures with reduced amplitude and longer wavelength. The structure of the Rheinsberg Trough is still visible as an area of reduced salt thickness. This changes after backstripping of the Upper Triassic Keuper layer. Fig. 9f shows the salt thickness distribution at the end of Mid–Triassic Muschelkalk, before the onset of the second extensional phase responsible for the development of the Rheinsberg Trough. The salt distribution is almost equilibrated at this time step with the exception of two large salt diapirs in the southern part of the basin. The existence of those two large structures in Middle Triassic times is, however, not well constrained as we had no seismic data from this area to prove our results. Fig. 9g shows the salt thickness distribution resulting from backstripping to the end of Late Permian Zechstein. The modelled initial thickness of the Zechstein salt indicates a NW–SE striking basin with the highest thickness of up to 2.5 km in the northwestern basin centre. This result is in good agreement with facies distribution studies (Kiersnowski et al., 1995) as well as with the thickness distribution of the underlying Lower Permian Rotliegend sediments (Plein, 1995; Scheck and Bayer, 1999) and the reconstructed initial thickness of the overlying Lower Triassic Buntsandstein (Fig. 8l).

6. Discussion and conclusions

The results, although preliminary, show that applying this method yields paleo-topographies which can be compared with facies patterns obtained by different geological methods. In addition, the short wavelength salt tectonics is filtered out and the temporal evolution of the major tectonic elements becomes visible, as we found by comparison of backstripping results with and without salt redistribution. The results indicate, that the assumption of a correlation between tectonic phases and phases of salt mobilisation is reasonable and consistent with geological data. Modelling of salt motion during basin deformation is a useful tool to test different geological hypotheses concerning erosion/uplift magnitudes. However, additional constraints are needed to consider the right timing of diapirism.

Our results support the conclusion that major salt movements took place during Late Triassic–Jurassic and during Late Cretaceous–Early Cenozoic as indicated in the overview (Fig. 10). The NNE–SSW oriented long axis of the Late Triassic to Jurassic subsidence centres points to E–W directed extension, which is consistent with the regional stress regime in North Central Europe at that time. Comparably, the WNW–ESE striking axes of salt cored anticlines due to Late Cretaceous–Early Cenozoic folding of the salt cover point to a NNE–SSW compression. The latter finding is also consistent with results from other basins of North Central Europe.

It is known that E–W directed crustal extension during Late Triassic times resulted in normal faulting of the salt basement and accelerated basement subsidence further west in the Glückstadt Graben, the Horn

Fig. 9. Comparison of salt distribution at different time steps. (a) Modelled present-day salt thickness [in m] showing tall and narrow diapirs in the southeastern part of the basin and small amplitude, large wavelength salt pillows in the NW. (b) Salt distribution after backstripping the Cenozoic showing that the salt structures in the central and northwestern part of the basin are restored. (c) Result of backstripping the Cenozoic and subsequent reloading of the system with the cover thickness reconstructed for the Late Cretaceous before inversion. Most of the piercing is restored, some salt pillows remain as well as a salt withdrawal zone in the area of the Rheinsberg Trough. Backstripping results for the beginning of Cretaceous (d), beginning of Jurassic (e), beginning of Keuper (f) and the end of Zechstein (g). The salt withdrawal zone in the area of the Rheinsberg Trough is successively closing and disappears in the result obtained for the beginning of Late Triassic (Keuper). For the end of Zechstein (g), we obtain a reconstructed map of initial salt thickness corresponding to a wide NW–SE oriented basin.

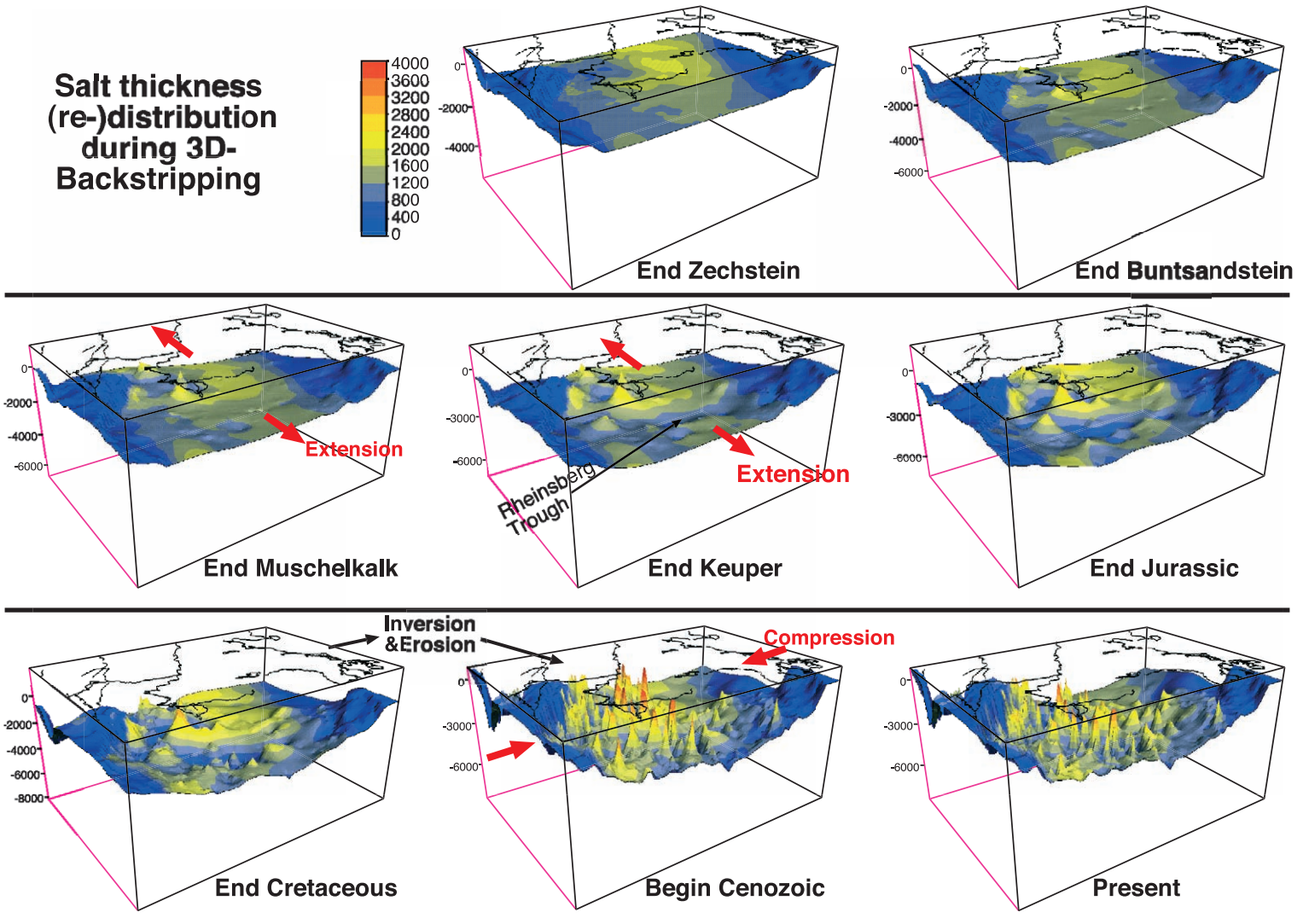

Fig. 10. Overview on the results of backstripping and salt redistribution for all time steps indicating that major changes in salt configuration took place in Late Triassic–Jurassic extension and during Late Cretaceous inversion. The deformation intensity is largest during Late Cretaceous inversion.

Graben and the Central Graben. In northeastern Germany, the magnitude of extension obviously was smaller. The Late Triassic, E–W directed extension leads to the formation of the Rheinsberg Trough in the salt cover but did not cause deformation of the salt basement. From this observation, we can conclude that the effective stress did not exceed the yield strength of the salt basement, but was high enough to provoke deformation of the viscous salt layer and its cover. Horizontal strain propagation may have occurred in the cover sediments of the salt layer from the more intensely deformed grabens in the west to the Rheinsberg Trough in the east. Thereby, the salt movement may have passively balanced the major part of extension as salt starts to deform already under very small differential stresses. In addition, initial salt mobilisation in the NEGB may have taken place in response to salt movements in the western part of the North German Basin, where basement faults demonstrate considerable amounts of crustal extension. This initial salt movement probably was re-enforced by a feedback mechanism envolving sediment downbuilding in rim synclines and salt withdrawal. Removing the load of the sediments in the Late Triassic to Jurassic Rheinsberg Trough results in the almost complete closure of the present-day hole in the salt layer due to salt flowing back into this hole. This means that the isostatic effects of the sediment load in the Rheinsberg Trough could largely explain the formation of the trough—an indication that the tectonic forces leading to beginning salt mobilisation were rather small during regional Late Triassic extension in the study area.

In contrast, strong deformation took place along the southern basin margin during the Late Cretaceous–Early Cenozoic phase of inversion leading to a present-day vertical basement offset of 5 km. This indicates that the tectonic forces responsible for this deformation have been of a considerable magnitude. For this phase, seismic data (Fig. 3; DEKORP-BASIN Research Group, 1999; Scheck et al., 2002) show that basement faulting occurs up to 50 km north of the main basement fault at the southern basin margin. However, the vertical offsets along the basement faults in this area are continuously decreasing with increasing distance to the main fault (Fig. 3a,b). In the salt and its cover, Late Cretaceous to Early Cenozoic compressive deformation affects almost the entire basin, leading to folding and faulting of the cover sediments. Line-length balancing of a Muschelkalk reflection, parallel to the direction of maximum compression (NNE–SSW) revealed that shortening in the Mesozoic salt cover amounts up to 3% (Scheck et al., 2002; Otto and Bayer, 2001). However, amplitudes and frequency of salt structures continuously decrease with increasing distance to the main basement fault at the southern basin margin. This indicates that strain was localised along the main fault system at the southern basin margin and was laterally transferred in the salt cover from the basin margin into the basin supported by viscous salt flow. A similar concept was proposed by Kossow et al. (2000) Our findings furthermore support the results of Letouzey et al. (1995), who also found strong indications for salt-related horizontal strain propagation in compressive settings.

6.1. Present limitations and outlook

Major limits of the method are in the context of the basic assumptions. Further development of the method is needed to include salt loss due to solution processes because these processes may be relevant for the salt mobilization history as recently demonstrated by Cartwright et al. (2001). Additional work is required to handle complex geometries like salt overhangs or mushroom-shaped diapirs. Furthermore, the restoration of the fault heaves in the salt basement is a future challenge to be worked on possibly by combining other restoration methods with our approach. Likewise, the output of the different restoration steps could serve as input for additional basin modelling methods like, for example, calculations of paleogeothermal fields and related hydrocarbon generation and/or migration. Finally, the results strongly depend on the quality of the structural model and on the initial, pre-piercing thicknesses used as input during diapir restoration. Therefore, it seems useful to have a tool allowing an automatic reconstruction of a range of initial cover thickness as in many basins little is known about the initial thickness distribution.

The method presented in this study is very useful in thin-skinned structural settings with salt as decoupling horizon and could be successfully applied in parts of the North Sea, in the Norwegian–Danish Basin and in the Polish Basin. A comparison of the decoupling phenomena related to salt movement un-

der changing stress fields across the Central European Basin System could shed new light on its evolution.

Acknowledgements

We are very grateful for the constructive comments of P. Krzywiec and M. Huuse who helped to improve the quality of this paper considerably. This project was funded by the Deutsche Forschungsgemeinschaft.

References

Badley, M.E., Price, J.D., Blackshall, L.C., 1989. Inversion, reactivated faults and related structures: seismic examples from the Southern North Sea. In: Cooper, M.A., Williams, G.D. (Eds.), Inversion Tectonics. Geol. Soc. Spec. Publ. Classics. The Geological Society of London, pp. 201–222.

Benek, R., Kramer, W., McCann, T., Scheck, M., Negendank, J.F.W., Korich, D., Huebscher, H., Bayer, U., 1996. Permo-Carboniferous magmatism and related subsidence of the NE German basin. Tectonophysics 266, 379–404.

Betz, D., Führer, F., Plein, E., 1987. Evolution of the Lower Saxony Basin. Tectonophysics 137, 127–170.

Bond, C.G., Kominz, M., 1984. Construction of tectonic subsidence curves for the Early Paleozoic miogeocline, southern Canadian Rocky Mountains: implications for subsidence mechanisms, age of breakup, and crustal thinning. Geol. Soc. Amer. Bull. 95, 155–173.

Brink, H.J., Duerschner, H., Trappe, H., 1992. Some aspects on the late and post-Variscan development of the northwestern German basin. Tectonophysics 207, 65–92.

Buchanan, P.G., Bishop, D.J., Hood, D.N., 1996. Development of salt related structures in the Central North Sea: results from section balancing. In: Alsop, G.I., Blundell, D.J., Davison, I. (Eds.), Salt Tectonics. Geological Society Special Publication, vol. 100, pp. 111–128.

Cartwright, J.A., 1989. The kinematics of inversion in the Danish Central Graben. In: Cooper, M.A., Williams, G.D. (Eds.), Inversion Tectonics. Geol. Soc. Spec. Publ. Classics. The Geological Society of London, pp. 153–176.

Cartwright, J., Stewart, S., Clark, J., 2001. Salt dissolution and salt related deformation of the Forth Approaches Basin, UK North Sea. Mar. Pet. Geol. 18, 757–778.

Clausen, O.R., Korstgård, J.A., 1996. Planar detaching faults in the southern Horn Graben, Danish North Sea. Mar. Pet. Geol. 13, 537–549.

Clausen, O.R., Pedersen, P.K., 1999. The Triassic structural evolution of the southern margin of the Ringkøbing-Fyn-High, Denmark. Mar. Pet. Geol. 16, 653–665.

Coward, M., Stewart, S., 1995. Salt-influenced structures in the Mesozoic–Tertiary cover of the southern North Sea, UK. In: Jackson, M.P.A., Roberts, D.G., Snelson, S. (Eds.), Salt Tectonics A Global Perspective. AAPG Mem., vol. 65, pp. 229–250.

Davison, I., Alsop, G.I., Blundell, D.J., 1995. Salt tectonics: some aspects of deformation mechanics. In: Alsop, G.I., Blundell, D.J., Davison, I. (Eds.), Salt Tectonics. Geological Society Special Publication, vol. 100, pp. 1–10.

DEKORP-BASIN Research Group, 1999. The deep structure of the NE German Basin—constraints on the controlling mechanisms of intracontinental basin development. Geology 27 (1), 55–58.

Demercian, S., Szatmari, S., Cobbold, P., 1993. Style and pattern of salt diapirs due to thin-skinned gravitational gliding, Campos and Santos Basins, Offshore Brazil. Tectonophysics 228, 393–433.

Giese, P., 1995. Main features of geophysical structures in Central Europe. In: Dallmeyer, R.D., Franke, W., Weber, K. (Eds.), Pre-Permian Geology of Central and Eastern Europe. Springer-Verlag, Heidelberg, pp. 7–25.

Hoffman, N., Stiewe, H., 1994. Neuerkenntnisse zur geologisch geophysikalischen Modellierung der Pritzwalker Anomalie im Bereich des Ostelbischen Massivs. Z. Geol. Wiss. 22 (1/2), 161–171.

Hooper, R.J., More, C., 1995. Evaluation of some salt related overburden structures in the UK southern North Sea. In: Jackson, D.G., Roberts, D.G., Snelson, S. (Eds.), Salt Tectonics A Global Perspective. AAPG Mem., vol. 65, pp. 251–259.

Hoth, K., Huebscher, H.-D., Korich, D., Gabriel, W., Enderlein, F., 1993. Die Lithostratigraphie der permokarbonischen Effusiva im Zentralabschnitt der mitteleuropäischen Senke. Geol. Jahrb. 36/11, 397–400.

Ismail-Zadeh, A.T., Talbot, C.J., Volozh, Y.A., 2001. Dynamic restoration of profiles across diapiric structures: numerical approach and its applications. Tectonophysics 337, 23–38.

Jaritz, W., 1987. The origin and development of salt structures in northwest Germany. In: Lerche, I., O'Brian, J.J. (Eds.), Dynamical Geology of Salt and Related Structures. Academic Press, Orlando, FL, pp. 479–493.

Kiersnowski, H., Paul, J., Peryt, T.M., Smith, D.B., 1995. Facies, paleogeography, and sedimentary history of the Southern Permian basin in Europe. In: Scholle, P., Peryt, T.M., Ulmer-Scholle, D.S. (Eds.), The Permian of Northern Pangea, vol. 1, pp. 119–136.

Kockel, F., 1995. Structural and paleogeographical development of the German North Sea sector, Berlin, Stuttgart. Beiträge zur Regionalen Geologie der Erde, vol. 26. Gebrüder Bornträger, Stuttgart.

Kockel, F. (Ed.), 1996. Geotektonischer Atlas von NW-Deutschland/Tectonic Atlas of NW-Germany 1:300 000. Compiled by: Baldschuhn, R., Frisch, U., Kockel, F. authors: Baldschuhn R., Best, G., Deneke, E., Frisch, U., Juergens, U., Kockel, F., Schmitz, J., Sattler-Kosinowski, S., Stancu-Kristoff, G., Zirngast, M. Bundesanstalt fuer Geowissenschaften und Rohstoffe, Hannover.

Kossow, D., 2002. Die kinematische Entwicklung des invertierten, intrakontinentalen Nordostdeutschen Beckens. Scientific Technical Report STR02/04, GeoForschungsZentrum Potsdam.

Kossow, D., Krawczyk, C., McCann, T., Strecker, M., Negendank, J.F.W., 2000. Style and evolution of salt pillows and related structures in the northern part of the northeast German basin. Int. J. Earth Sci, pp. 652–664.

Koyi, H., Talbot, C.J., Tørudbakken, B.O., 1993. Salt diapirs of the southwest Nordkapp Basin: analogue modelling. Tectonophysics 228, 167–187.

Letouzey, J., Coletta, B., Vially, R., 1995. Evolution of salt-related structures in compressional settings. In: Jackson, M.P.A., Roberts, D.G., Snelson, S. (Eds.), Salt Tectonics A Global Perspective. AAPG Mem., vol. 65, pp. 41–60.

Lokhorst, A. (Ed.), 1998. NW European Gas Atlas—Composition and Isotope ratios of Natural Gases, Gis application on CD by the British Geological Survey, Bundesanstalt für Geowissenschaften und Rohstoffe, Danmarks og Gronlands Geologiske Undersogelse, Nederlands Instituut voor Toegepaste Geowetenschappen, Panstwowy Instytut Geologiczny, European Union.

Meinhold, R., Reinhardt, H.-G., 1967. Halokinese im nordostdeutschen Tiefland. Ber. Dtsch. Ges. Geol. Wiss., A Geol. Paläontol. 12 (3/4), 329–353.

Musstow, R., 1976. Lithologisch-Paläogeographische Karte der DDR, Oberkreide (Cenoman-Maastricht) 1:500000.

Nalpas, T., Brun, J.P., 1993. Salt flow and diapirism related to extension at crustal scale. Tectonophysics 228, 349–362.

Odonne, F., Costa, E., 1993. Relationships between strike-slip movement and fold trends in thin-skinned tectonics: analogue models. Tectonophysics 228, 383–391.

Otto, V., Bayer, U., 2001. Inversion related features along the southern margin of the Northeast German Basin. EUG European Union of Geosciences XI, 8.–12. April 2001, Strasbourg, France, Journal of Conference Abstracts 6, Strasbourg, France, LS05:SUpm35:F2.

Plein, E., 1995. Stratigraphie von Deutschland I, Norddeutsches Rotliegendbecken Rotliegend-Monographie. Cour. Forsch.-Inst. Senckenb. 183, 1–193 (Frankfurt am Main).

Podlachikov, Y., Talbot, C., Poliakov, A.N.B., 1993. Numerical models of complex diapirs. Tectonophysics 228, 189–198.

Poliakov, A.N.B., Podlachikov, Y., Talbot, C., 1993. Initiation of salt diapirs with frictional overburdens: numerical experiments. Tectonophysics 228, 199–210.

Rabbel, W., Förste, K., Schulze, A., Bittner, R., Röhl, J., Reichert, J.C., 1995. A high-velocity layer in the lower crust of the north German basin. Terra Nova 7, 327–337.

Remmelts, G., 1995. Fault-related tectonics in the southern North Sea, The Netherlands. In: Jackson, M.P.A., Roberts, D.G., Snelson, S. (Eds.), Salt Tectonics A Global Perspective. AAPG Mem., vol. 65, pp. 261–272.

Rowan, M.G., 1993. A systematique technique for the sequential restoration of salt structures. Tectonophysics 228, 331–348.

Schäfer, F., Griffiths, P., Osborn, R., 1998. Balancing salt structures in 3D. Tagungsband zum 18. DGMK-Mintrop-Seminar, Ruhr-Universität Bochum, 69–107.

Scheck, M., Bayer, U., 1997. Configuration of the crust below the intracratonic northeast German basin: preliminary modelling results. Terra Nostra 97/11, 121–125.

Scheck, M., Bayer, U., 1999. Evolution of the northeast German basin—Inferences from a 3D structural model and subsidence analysis. Tectonophysics 313, 145–69.

Scheck, M., Bario-Alvers, L., Bayer, U., Götze, H.-J., 1999. Density structure of the Northeast German Basin: 3D modelling along the DEKORP Line BASIN96. Phys. Chem. Earth, Part A 24, 221–230.

Scheck, M., Bayer, U., Otto, V., Lamarche, J., Banka, D., Pharaoh, T., 2002. The Elbe Fault System in North Central Europe—a basement controlled zone of crustal weakness. Tectonophysics 360, 281–299.

Schultz-Ela, D., Jackson, M.P.A., Vendeville, B., 1993. Mechanics of active salt diapirism. Tectonophysics 228, 275–312.

Schwab, G., 1985. Paläomobilität der Norddeutsch-Polnischen Senke. Unpublished thesis B, Akademie der Wissenschaften der DDR, Potsdam, Germany.

Sclater, J.G., Christie, P.A.F., 1980. Continental stretching: an explanation of the post-Mid-Cretaceous subsidence of the Central North Sea basin. J. Geophys. Res. 85, 3711–3739.

Steckler, M.S., Watts, A.B., 1978. Subsidence of the Atlantic-type continental margin off New York. Earth Planet. Sci. Lett. 41, 1–13.

Stewart, S.A., Harvey, M.J., Otto, S.C., Weston, P.J., 1996. Influence of salt on fault geometry: examples from the UK salt basins. In: Alsop, G.I., Blundell, D.J., Davison, I. (Eds.), Salt Tectonics. Geological Society Special Publication, vol. 100, pp. 175–202.

Van Keken, P.E., Spiers, C.J., Van den Berg, A.P., Muyzert, E.J., 1993. The effective viscosity of rocksalt: implementation of steady-state creep laws in numerical models of salt diapirism. Tectonophysics 225, 457–476.

Van Wees, J.D., Stephenson, R.A., Ziegler, P.A., Bayer, U., McCann, T., Dadlez, R., Gaupp, R., Narkiewicz, M., Bitzer, F., Scheck, M., 2000. On the origin of the Southern Permian Basin, Central Europe. Mar. Pet. Geol. 17, 43–59.

Vendeville, B.C., Jackson, M.P.A., 1992. The rise of diapirs during thin-skinned extension. Mar. Pet. Geol. 9, 331–353.

Vendeville, B.C., Hongxing, G., Jackson, M.P.A., 1995. Scale models of salt tectonics during basement-involved extension. Pet. Geosci. 1, 179–183.

Whitefield, C., Jaffri, F., Griffiths, P.A., Jones, S., 1999. 3D computer modeling and restoration of Gulf of Mexico-type allochtonous salt structures. American Association of Petroleum Geologists, 1999 Annual Meeting, Annual Meeting Expanded Abstracts. American Association of Petroleum Geologists, San Antonio, TX, p. A150.

Yin, H., Groshong Jr., R.H., 1999. Salt piercement structures, 3-D kinematic modeling and balanced cross-sections; preliminary results. Geological Society of America, 1999 Annual Meeting, Abstracts with Programs, vol. 31; 7. Geological Society of America, San Antonio, TX, p. 126.

Zentrales Geologisches Institut—ZGI, Nöldeke W. (wissenschaftl. Redaktion), 1968–1990. Lithologisch-Paläogeographische Karte der DDR, VEB Kartographischer Dienst Potsdam.

Ziegler, P., 1990. Geological Atlas of Western and Central Europe, 2nd ed. Shell International Petroleum Mij, The Hague, pp. 1–239. Distributed by Geol. Soc. Publ. House Bath.

Zirngast, M., 1996. The development of the Gorleben salt dome (northwest Germany) based on quantitative analysis of peripheral sinks. In: Alsop, G.I., Blundell, D.J., Davison, I. (Eds.), Salt Tectonics. Geological Society Special Publication, vol. 100, pp. 203–226.